



Sediments as Sentinels of Pollution Episodes in the Middle Estuary of the Tinto River (SW Spain)

Luis Miguel Cáceres ¹, Francisco Ruiz ^{1,*}, Javier Bermejo ², Lucía Fernández ²,
María Luz González-Regalado ¹, Joaquín Rodríguez Vidal ¹, Manuel Abad ³, Tatiana Izquierdo ³,
Antonio Toscano ¹, Paula Gómez ¹ and Verónica Romero ¹

¹ Departamento de Ciencias de la Tierra, Universidad de Huelva, 21071 Huelva, Spain; mcaceres@uhu.es (L.M.C.); jrvidal@uhu.es (J.R.V.)

² Departamento de Historia, Geografía y Antropología, Universidad de Huelva, 21071 Huelva, Spain; javier.bermejo@dhis1.uhu.es (J.B.); lucia.fernandez@dhga.uhu.es (L.F.)

³ Departamento de Biología y Geología, Física y Química Inorgánica, Universidad Rey Juan Carlos, 28933 Móstoles, Spain; tatiana.izquierdo@urjc.es

* Correspondence: ruizmu@uhu.es

Abstract: Estuaries are excellent environments for identifying pollution episodes that have affected river basins, as their sediments are the final destination of some of the pollutants. This paper studies the geochemical evolution of five elements (As, Co, Cu, Pb, Zn) in a core extracted from the middle estuary of the Tinto River (SW Spain). The results are based on facies interpretation, ICP atomic emission spectrometry analysis, the application of a regional background to obtain the geoaccumulation index and dating. The main objective of this communication is the detection of natural or anthropogenic pollution episodes in the middle estuary of the Tinto River (SW Spain). Four pollution episodes have been detected: (1) ~5.8 cal. kyr BP, probably caused by natural acid rock drainage processes derived from the oxidation of the Iberian Pyritic Belt deposits found in its drainage basin; (2) 4.7–4.5 kyr BP, coming from the first mining activities and characterized by a significant increase in the concentrations of the five elements analyzed; (3) 1850–1960 interval, coinciding with intensive mining and characterized by increasing values of As and, to a lesser extent, Pb (intensive mining); and (4) the second half of the 20th century, with high element concentrations deduced from the geoaccumulation index. This communication can serve as an example for assessing the impact of different types of pollution in estuarine environments.

Keywords: sediment; pollution; core; geoaccumulation index; estuary; SW Spain



Citation: Cáceres, L.M.; Ruiz, F.; Bermejo, J.; Fernández, L.; González-Regalado, M.L.; Vidal, J.R.; Abad, M.; Izquierdo, T.; Toscano, A.; Gómez, P.; et al. Sediments as Sentinels of Pollution Episodes in the Middle Estuary of the Tinto River (SW Spain). *Soil Syst.* **2023**, *7*, 95. <https://doi.org/10.3390/soilsystems7040095>

Academic Editor: Manfred Sager

Received: 14 September 2023

Revised: 20 October 2023

Accepted: 21 October 2023

Published: 24 October 2023



Copyright: © 2023 by the authors. Licensee MDPI, Basel, Switzerland. This article is an open access article distributed under the terms and conditions of the Creative Commons Attribution (CC BY) license (<https://creativecommons.org/licenses/by/4.0/>).

1. Introduction

Numerous anthropogenic activities (e.g., industrial effluents, mining waste, agricultural residues, urban inputs), the natural erosion of geological formations or even high-energy events (river floods, storms, tsunamis, etc.) leave their mark on the geochemical levels of sediments and soils [1–7]. One of the most common effects is the increase in concentrations of certain elements, among which heavy metals are commonly used as a reference to measure the level of pollution [8–11]. To determine the heavy metal contamination in a soil or sediment, various indices are often used, such as the enrichment factor (EF) or the geoaccumulation index (I_{geo}) [12–14]. The latter index requires a regional background in order to calculate the degree of contamination, which may be unique for each metal regardless of grain size (e.g., [15–17]), or may include a differentiation between sandy and muddy sediments [18].

Estuaries are often the final repositories of many of these natural processes or human actions, as they often contain the inputs of heavy metals produced in their river basins at present or in the past [19–21]. In the last few years, numerous investigations have focused on

the historical heavy metal pollution of these environments, based on geochemical studies of continuous sediment cores [22–24]. Some of them have applied the geoaccumulation index to detect pollution episodes and, in conjunction with radiocarbon dating and historical data, to pinpoint the time interval in which they occurred [25,26].

The main objective of this short communication is the detection of natural or anthropogenic pollution episodes in a continuous sediment core extracted from the middle estuary of the Tinto River (SW Spain), based on the vertical geochemical variations and the application of the regional geoaccumulation index to five elements. The results obtained will be compared with previous paleoenvironmental reconstructions and historical mining data to identify the age of these episodes and their importance according to the degree of contamination deduced. Furthermore, it is intended that these results can be used to compare the importance of these episodes or be extrapolated in the future to analyses of recent sediments from this estuary.

2. Materials and Methods

2.1. Study Area

The Tinto River is a small stream that flows through the southwest of Spain and forms a large estuary together with the Odiel River at its mouth in the Atlantic Ocean, surrounded by Neogene–Pleistocene formations (Figure 1A,B). The hydrodynamics of this estuary are tidally dominated, as river discharges are very rare and vary from minimum flows during very dry years to about 350 Hm³ in rainy years [27]. The tidal regime is mesotidal (2.1 m), with a low diurnal inequality [28].

This estuary can be divided into three sectors, depending on the interaction between the river and tidal inputs [29]: (i) fluvial estuary, composed of numerous braided channels; (ii) middle estuary, with numerous marshes that come to form small islands (e.g., Figure 1B: Bacuta Island); and (iii) marine estuary, with a central island (Figure 1B: Saltés Island), two main channels (Padre Santo channel, Punta Umbría channel) and two sandy spits (Punta Arenillas, Punta Umbría) that partially protect it. In the marine estuary, wave energy is medium, and 75% of the waves do not exceed 0.5 m in height [30]. The coastal drift currents are oriented towards the east, with a high annual transport of sediment ($1.8 - 3 \times 10^5 \text{ m}^3$) [31,32], and have historically favored the development of the two spits and the progressive closure of the innermost parts of the estuary.

2.2. Historical Pollution

Southwest Spain is part of the Iberian Pyritic Belt, one of the most important metallogenic provinces in Europe, which includes some of the largest massive sulfide deposits in the world. These giant deposits have been exploited for 5000 years within the Tinto River drainage basin [27], with important mining activity during the Roman period (2100–1700 yr BP) and especially in the last 150 years, with an intensive extraction of pyrite and minor quantities of gold and silver. Currently, the waters of the Tinto River suffer from acid mine drainage, due to this age-old mining activity and to the heavy-metal-rich inputs from the washing of the waste dumps generated [33].

In addition, this estuary has been affected by discharges from two industrial concentrations located on its banks since the 1960s (Figure 1B), made up of copper producers, fertilizer factories and refineries, among others. As a final result of these mining–industrial pollutant inputs, the surface sediments of the Tinto–Odiel estuary are among the most polluted in the world, with very high concentrations of As (up to 3000 mg kg^{−1}), Cu (up to 4415 mg kg^{−1}), Pb (up to 10,400 mg kg^{−1}) and Zn (up to 5280 mg kg^{−1}) in its surface sediments [18,34]. Since 1985, this zone has come under a corrective plan for the control of industrial waste disposal.

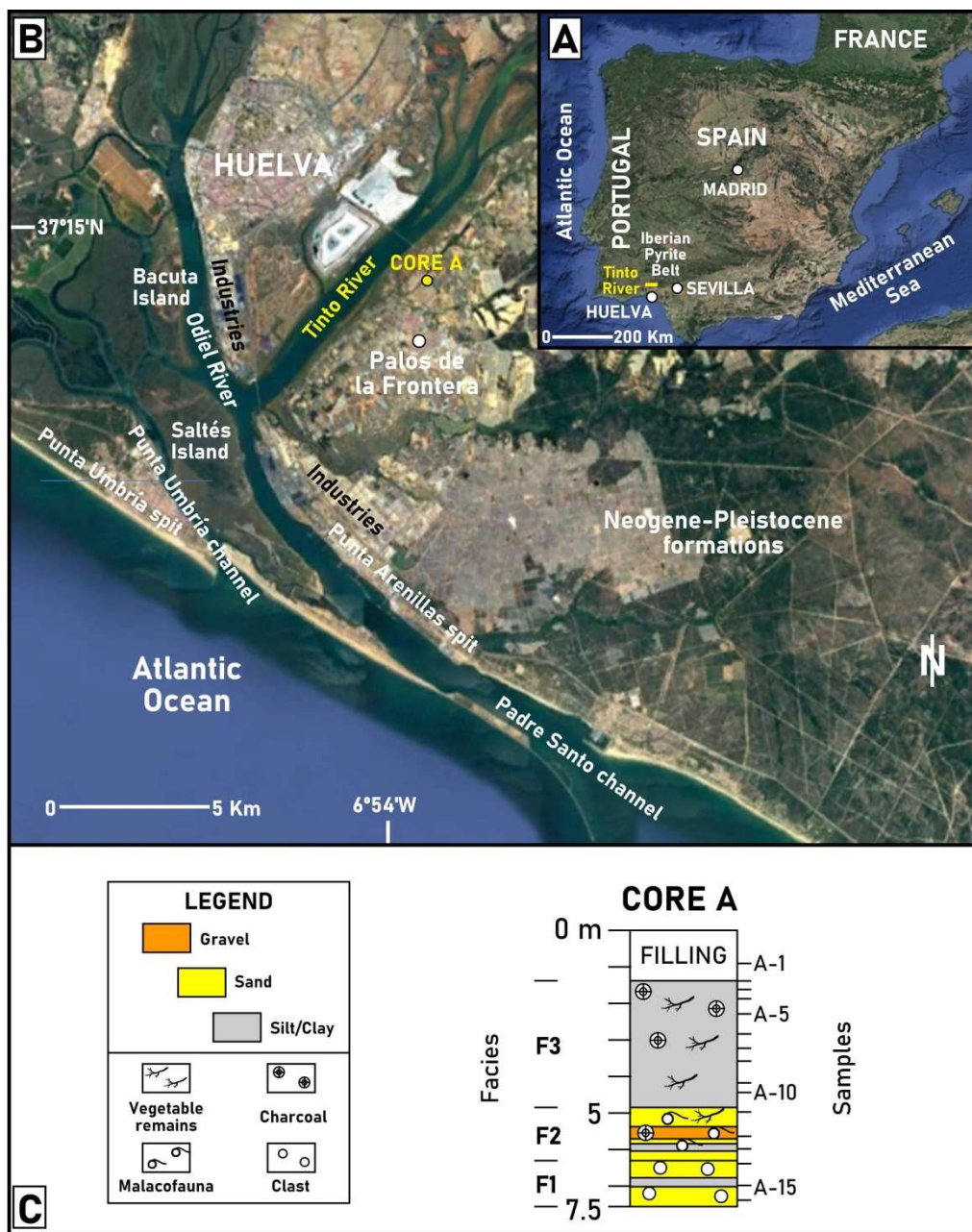


Figure 1. (A) Location of the Tinto–Odiel estuary. (B) Synthetic geomorphological map of the Tinto–Odiel estuary, with location of core A. (C) Log of core A, including sedimentary facies and sampling. (A,B) Courtesy Google Earth.

2.3. Coring, Sampling and Holocene Paleoenvironmental Evolution

Core A (Figure 1B,C; 7.5 m depth; 37°14'06" N; 6°53'54" W) was extracted in the middle estuary of the Tinto River by usual rotary drilling techniques, with an almost continuous recovery of sediment and a barrel diameter of 11.6 cm. Its location was selected in an area away from the main channel of the Tinto River, only flooded during high tides and not subject to the erosive action of the occasional large flows that characterize this highly seasonal river. Sixteen samples (2 cm thickness) were obtained, with a distribution of samples linked to (a) the presence of different sedimentary facies, (b) the definition of its limits and (c) the visual distribution of bioclasts in the core. The Holocene paleoenvironmental reconstruction of this core was inferred by [35], with basal alluvial sands (Figure 1C: facies F1), bioclastic sands and gravels from the marine flood of this area during the MIS-1 transgression (F2) and upper muddy marsh deposits (F3).

2.4. Chemical Analysis

The chemical analysis of sixteen sediment samples was performed and certified by MS Analytical (Langley, BC, Canada). Samples were collected manually by hand picking. They were individually crushed and subsequently ground into powder using an agate mortar. The concentrations of five elements (As, Co, Cu, Pb, Zn) were determined by ICP atomic emission spectrometry (total digestion with concentrated acids), with less than 5% variation between different replicate samples and quality control based on more than 30 references (e.g., OREAS 904). In these samples, detection limits varied between 0.01 mg kg⁻¹ (e.g., Co) and 2 mg kg⁻¹ (e.g., Zn).

2.5. Background and Geoaccumulation Index

A regional background of this estuary was obtained by [36] for both unpolluted sandy and muddy sediments of the Tinto–Odiel estuary. This background was applied to obtain the geoaccumulation index of the extracted sediments, according to the following formula:

$$I_{\text{geo}} = \log_2 C_n / 1.5 \times B_n,$$

where C_n is the concentration of an element in a given sample and B_n is the background of that element for the grain size of that sample (e.g., sand or mud). This background differentiates sandy (S) and muddy (M) sediments: As (S: 6.8 mg kg⁻¹; M: 7.3 mg kg⁻¹), Co (S: 4.2 mg kg⁻¹; M: 6.8 mg kg⁻¹), Cu (S: 13.1 mg kg⁻¹; M: 13 mg kg⁻¹), Pb (S: 4.3 mg kg⁻¹; M: 15.4 mg kg⁻¹) and Zn (S: 15.9 mg kg⁻¹; M: 39 mg kg⁻¹).

The pollution classes originally proposed by [37] were slightly modified as follows: unpolluted (UP; $I_{\text{geo}} < 0$), very low pollution (VLP; $0 < I_{\text{geo}} < 1$), low pollution (LP; $1 < I_{\text{geo}} < 2$), moderately polluted (MP; $2 < I_{\text{geo}} < 3$), highly polluted (HP; $3 < I_{\text{geo}} < 4$), very highly polluted (VHP; $4 < I_{\text{geo}} < 5$) and strongly polluted (SP; $I_{\text{geo}} > 5$).

2.6. Dating

Two dates of core A were produced at the National Center of Accelerators (Sevilla, Spain). These dates were calibrated using CALIB version 8.2, and the final results correspond to calibrated ages using 2σ intervals.

3. Results and Discussion

3.1. Facies, Geochemistry and Dating

The basal alluvial sandy–muddy deposits of this core (F1; 7.5–6.3 m depth; samples A-16 to A-14) have very low concentrations of most of the elements studied, even lower than the regional background (Table 1). They were deposited during the Middle Holocene, according to the dating obtained near the boundary between F1 and F2 (Figure 1C and Table 2; sample A-13; ~5.8 cal. kyr BP). The bioclastic sediments of this last facies (6.3–4.9 m depth; samples A-13 to A-11; ~5.8–5 cal. kyr BP) were deposited during the flooding of this area due to the MIS-1 transgression. A first pollution level was detected near the base of this facies (sample A-13: ~5.8 cal. kyr BP), with a noticeable increase in the concentrations of Cu (from 9.5 mg kg⁻¹ to 39 mg kg⁻¹), Pb (from 11.1 mg kg⁻¹ to 74.1 mg kg⁻¹) and Zn (from 25 mg kg⁻¹ to 93 mg kg⁻¹). The age of this level would indicate early natural pollution, as mining did not begin in this area until some thousand years later [27,38]. The origin of this first contamination is unknown, although it could come from the natural oxidation of the sulfides and formation of the gossans of the Iberian Pyritic Belt by acid rock drainage processes, which started more than 24 million years ago in this area [39]. Metals from the washing of these deposits would have been transported to the Tinto estuary and deposited in core A when its environment was flooded during the Holocene transgression. This episode has been detected in other cores of the Tinto estuary [40], and this research confirms this first natural pollution.

Table 1. Geochemistry of core A (in mg kg⁻¹). Bold: three highest values of each element.

Sample	Depth (m)	Sediment	Facies	Interpretation	As	Co	Cu	Pb	Zn
A-1	0.9	Sand	Filling	Recent filling	7	3.7	21	14.7	30
A-2	1.4	Mud	F4	Marsh	43.8	13.1	284.4	98	539
A-3	1.6	Mud	F4	Marsh	39.3	12.7	27.5	37.9	88
A-4	1.9	Mud	F4	Marsh	36.7	14.1	23.8	23.2	85
A-5	2.3	Mud	F4	Marsh	18.3	12	20.3	22.1	87
A-6	2.8	Mud	F4	Marsh	19.2	12.1	22.7	27.9	89
A-7	3.3	Mud	F4	Marsh	17.2	10.3	15.7	40.6	68
A-8	3.6	Mud	F4	Marsh	22.2	11.5	22.8	18.6	87
A-9	4.2	Mud	F4	Marsh	30.1	12.4	51.8	46.9	107
A-10	4.5	Mud	F4	Marsh	18.2	9.7	18.5	17.8	69
A-11	5	Sand	F2	MIS-1 transgression	12.3	5.9	11.7	12.4	44
A-12	5.7	Gravel	F2	MIS-1 transgression	8.5	3.9	8.4	10	28
A-13	6	Mud	F2	MIS-1 transgression	27.3	10.6	39	74.1	93
A-14	6.4	Sand	F1	Alluvial	4.8	4.4	9.5	11.1	25
A-15	7	Mud	F1	Alluvial	6.7	6.4	10.9	14.9	33
A-16	7.4	Sand	F1	Alluvial	7.2	5.8	21.3	10.6	34

Table 2. Radiocarbon database.

Sample	Laboratory Number	Material	$\delta^{13}\text{C}$ (%)	Uncalibrated Age BP	Calibrated Age BP	Mean Calibrated Age (kyr BP)
A-12	CNA-4272	Organic matter	-22.6	6467 ± 32	5483–5368	5.4
A-13	CNA-4274	Shell	-1.3	5428 ± 33	5892–5711	5.8

The second pollution level was detected in the marshy muds collected near the base of F3 (Table 1: sample A-9), with some of the highest values of Cu (51.8 mg kg⁻¹), Pb (46.9 mg kg⁻¹) and Zn (107 mg kg⁻¹) of core A and increasing concentrations of As and Co. According to the average sedimentation rates (1.7–2 mm yr⁻¹) calculated by [41] in this estuary around 5000–4000 yr BP and the aforementioned dating, this new episode would have taken place approximately between ~4.7 kyr BP and ~4.5 kyr BP, coinciding with the development of the first mining and metallurgical works in this area [38]. This first episode of anthropogenic contamination has been detected in numerous cores in the Tinto River estuary e.g., [35,40].

The concentrations of the five elements decrease between 4.2 m depth and 2.3 m depth, with a further increase in As (from 18.3 mg kg⁻¹ to 36.9–39.3 mg kg⁻¹) and, to a lesser extent, Pb (up to 37.9 mg kg⁻¹) observed between 1.9 and 1.6 m depth. This third pollution episode is associated with the start of intensive mining in the Tinto River basin from the second half of the 19th century to 1960. This increasing trend is confirmed at 1.4 m depth (e.g., the surface of core A before the recent anthropogenic filling), with the maximum values of all five elements, especially Cu (284.4 mg kg⁻¹), Pb (98 mg kg⁻¹) and Zn (539 mg kg⁻¹). This fourth episode would correspond to the conjunction of this intensive mining and inputs from nearby industrial complexes during the second half of the 20th century, which have caused strong pollution in the recent sediments of the Tinto–Odiel estuary [42,43]. These high values confirm this last episode as the most important in the geochemical history of the middle estuary of the Tinto River. Transit to the overlying artificial filling is evidenced by the presence of unpolluted fine sands in the upper 1.3 m of this core (Table 1: sample A-1).

3.2. Geoaccumulation Index and Pollution Episodes

These four episodes are also detected when I_{geo} is applied to the concentrations of the five elements (Figure 2). The first episode (~5.8 cal. kyr BP) is characterized by the transition from UP (As, Co, Cu) or VLP (Pb) sediments to VLP (Co) or LP (As, Cu, Pb)

sediments. These four elements also show similar variations in their pollution class during the second episode (~4.7–4.5 kyr BP), most marked for Pb (from UP to LP) and to a lesser extent for As (from VLP to LP).

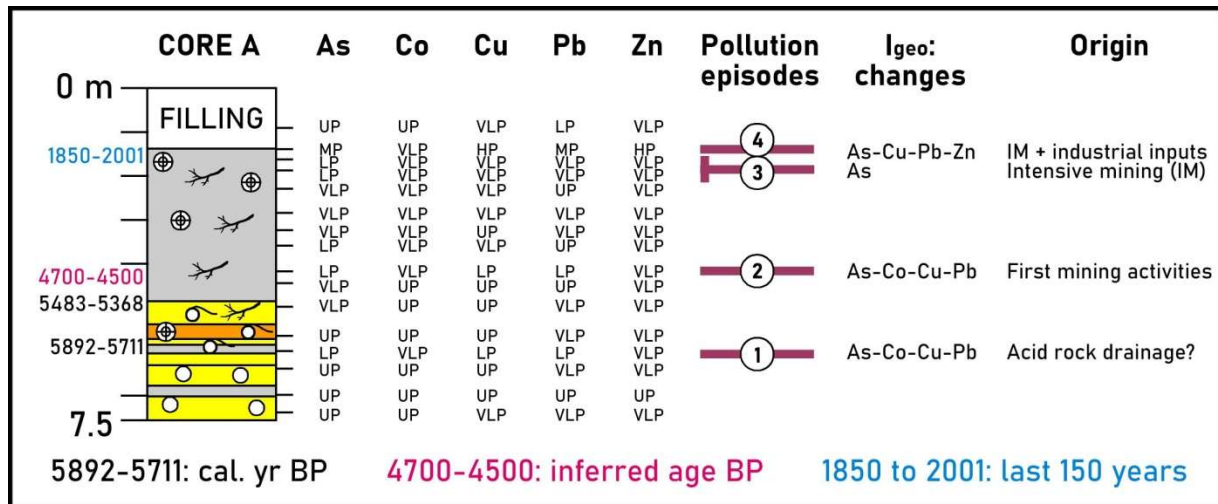


Figure 2. Application of I_{geo} to core A. For legend, see Figure 1.

The third episode (~1850–1960) is mainly defined by As (from VLP to LP), although an increase in the concentration of most of the other elements is observed (see previous subsection). The fourth episode (~1960–2000) is clearly the most important, with the presence of MP (As, Pb) to HP (Cu, Zn) sediments. Consequently, this last polluting episode is the most important in the geochemical history of the Tinto–Odiel estuary, as evidenced by the analysis of other sediment cores extracted in this area [35,44,45].

A final thought is needed on the calculation of the geoaccumulation index. It is a simple method to define the degree of contamination of a soil or sediment, but its formula includes a factor (1.5; see Section 2.5) because of possible variations in the background data due to different lithologies. Since heavy metals tend to concentrate in finer sediments, it would be advisable to use a background for each lithology (sand, silt, clay), if possible. On the other hand, the use of this multiplying factor in the denominator of the I_{geo} should be considered in the future, depending on the degree of lithification of sediment in estuaries, as it significantly increases the concentration of an element above which sediments are considered as contaminated.

4. Conclusions

The joint application of geochemical analysis and the geoaccumulation index has proved to be an effective tool for detecting pollution episodes in the middle estuary of the Tinto River (SW Spain), in conjunction with historical data on mining activities in this area. Four episodes have been distinguished, characterized by an increase in the concentration of the elements studied and their geochemical classes based on I_{geo} . The first recorded pollution was of natural origin and coincided with the flooding of this estuary during the Holocene transgression. The next three episodes are linked to the start of mining activities, a period of intensive mining, and the coincidence of intensive mining and the discharge of highly polluted industrial effluents into the estuary. The application of this background can be useful for determining the degree of contamination of the sediments of this estuary in relation to possible new sources of pollution, and the concentrations obtained can be used as a reference for assessing their importance in relation to the historical episodes referred to in this communication.

Author Contributions: All authors have participated in all stages of the paper. All authors have read and agreed to the published version of the manuscript.

Funding: This study was mainly financed by the Palos de la Frontera Council. It was also carried out through the following projects: (a) DGYCIT project CTM2006-06722/MAR; (b) DGYCIT project CGL2006-01412; (c) Roman cities of the Baetica, CORPVS VRBIVM BAETICARVM (I) (CUB) (Andalusian Government); (d) From the Atlantic to the Tyrrhenian, the Hispanic ports and their commercial relations with Ostia Antica, DEATLANTIR II—HAR2017-89154-P (Plan Nacional de I + D + i); and (e) FEDER 2014–2020 project UHU-1260298. Other funds have come from the Andalusian Government (groups HUM-132, RNM-238, and RNM-293). It is a contribution to the Research Center in Historical, Cultural and Natural Heritage (CIPHCHN) of the University of Huelva.

Institutional Review Board Statement: Not applicable.

Informed Consent Statement: Not applicable.

Data Availability Statement: Data are available upon request to the corresponding author.

Conflicts of Interest: The authors declare no conflict of interest.

References

1. Chagué-Goff, C.; Szczucinski, W.; Shinozaki, T. Applications of geochemistry in tsunami research: A review. *Earth-Sci. Rev.* **2017**, *165*, 203–244. [\[CrossRef\]](#)
2. Silva, H.F.; Silva, N.F.; Oliveira, C.M.; Matos, M.J. Heavy Metals Contamination of Urban Soils—A Decade Study in the City of Lisbon, Portugal. *Soil Syst.* **2021**, *5*, 27. [\[CrossRef\]](#)
3. Chebykina, E.; Abakumov, E.; Shamilishvilly, G.; Kouzov, S. Soil Diversity of the Island of Gogland in the Gulf of Finland: History of Land Development and Current Status. *Soil Syst.* **2022**, *6*, 85. [\[CrossRef\]](#)
4. Mangas-Suarez, M.; Garcia-Ordiales, E.; Pérez, J.A.; Álvarez, R.; Villa, A.; Ordoñez, A.; Roqueñí, N. Enrichment of Metals in the Sediments of an Industrially Impacted Estuary: Geochemistry, Dispersion and Environmental Considerations. *Appl. Sci.* **2022**, *12*, 10998. [\[CrossRef\]](#)
5. Papadimou, S.G.; Kantzou, O.-D.; Chartodiplomenou, M.-A.; Golia, E.E. Urban Soil Pollution by Heavy Metals: Effect of the Lockdown during the Period of COVID-19 on Pollutant Levels over a Five-Year Study. *Soil Syst.* **2023**, *7*, 28. [\[CrossRef\]](#)
6. Nassiri, O.; Rhoujjati, A.; Moreno-Jimenez, E.; Hachimi, M.L.E.L. Environmental and Geochemical Characteristics of Heavy Metals in Soils Around the Former Mining Area of Zeïda (High Moulouya, Morocco). *Water Air Soil Pollut.* **2023**, *234*, 110. [\[CrossRef\]](#)
7. Pereira, J.G.; Raikar, S.S.; Bhatti, A.G.; Fatarpekar, P.G.; Nasnodkar, M.R. Metal bioavailability, bioaccumulation, and toxicity assessment through sediment and edible biota from intertidal regions of the Aghanashini Estuary, India. *Mar. Environ. Res.* **2023**, *191*, 106172. [\[CrossRef\]](#)
8. Niu, S.; Xia, Y.; Yang, C.; Liu, C. Impacts of the steel industry on sediment pollution by heavy metals in urban water system. *Environ. Pollut.* **2023**, *335*, 122364. [\[CrossRef\]](#)
9. Hossain, M.B.; Sultana, J.; Pingki, F.H.; Nur, A.; Mia, M.S.; Bakar, M.A.; Yu, J.; Paray, B.A.; Arai, T. Accumulation and contamination assessment of heavy metals in sediments of commercial aquaculture farms from a coastal area along the northern Bay of Bengal. *Front. Environ. Sci.* **2023**, *11*, 1148360. [\[CrossRef\]](#)
10. Hamarashid, R.A.; Fiket, Ž.; Mohialdeen, I.M.J. Environmental Impact of Sulaimani Steel Plant (Kurdistan Region, Iraq) on Soil Geochemistry. *Soil Syst.* **2022**, *6*, 86. [\[CrossRef\]](#)
11. Rashid, A.; Schutte, B.J.; Ulery, A.; Deyholos, M.K.; Sanogo, S.; Lehnhoff, E.A.; Beck, L. Heavy Metal Contamination in Agricultural Soil: Environmental Pollutants Affecting Crop Health. *Agronomy* **2023**, *13*, 1521. [\[CrossRef\]](#)
12. Kroeksakul, P.; Ngamniyom, A.; Silprasit, K.; Singhaboot, P. Relationship between Potential Trace Elements Contamination in Sediment and Macrofauna in the Upper Gulf of Thailand. *J. Environ. Public Health* **2023**, *2023*, 4231930. [\[CrossRef\]](#)
13. Kumar, V.; Bhatti, R.C.; Kaur, R.; Singh, S.; Nirmala, C.; Singh, A.N. Comparative Geo-Accumulation Index of Heavy Metal Concentration in the Urban Soils of Chandigarh and Baddi Areas under Industrial Activities in A Lower Shiwalik Region, India. *Eur. Chem. Bull.* **2023**, *12*, 937–953. [\[CrossRef\]](#)
14. Fadlillah, L.N.; Utami, S.; Rachmawati, A.A.; Jayanto, G.D.; Widyastuti, M. Ecological risk and source identifications of heavy metals contamination in the water and surface sediments from anthropogenic impacts of urban river, Indonesia. *Heliyon* **2023**, *9*, e15485. [\[CrossRef\]](#)
15. Parvez, M.S.; Nawshin, S.; Sultana, S.; Hossain, M.S.; Rashid Khan, M.H.; Habib, M.A.; Nijhum, Z.T.; Khan, R. Evaluation of Heavy Metal Contamination in Soil Samples around Rampal, Bangladesh. *ACS Omega* **2023**, *8*, 15990–15999. [\[CrossRef\]](#) [\[PubMed\]](#)
16. Zaakour, F.; Kholaiq, M.; Khouchlaa, A.; El Mjiri, I.; Rahimi, A.; Saber, N. Assessment of Heavy Metal Contamination Using Pollution Index, Geo-Accumulation Index, and Potential Ecological Risk Index in Agricultural Soil—A Case Study in the Coastal Area of Doukkala (Morocco). *Ecol. Eng. Environ. Technol.* **2023**, *24*, 38–44. [\[CrossRef\]](#) [\[PubMed\]](#)
17. Kahangwa, C.A. Application of Principal Component Analysis, Cluster Analysis, Pollution Index and Geoaccumulation Index in Pollution Assessment with Heavy Metals from Gold Mining Operations, Tanzania. *J. Geosc. Environ. Protect.* **2022**, *10*, 303–317. [\[CrossRef\]](#)

18. Ruiz, F. Trace metals in estuarine sediments from the southwestern Spanish coast. *Mar. Pollut. Bull.* **2001**, *42*, 481–489. [[CrossRef](#)]
19. Li, H.; Gu, Y.; Liang, R.; Wang, Y.; Jordan, R.W.; Wang, L.; Jiang, S. Heavy metals in riverine/estuarine sediments from an aquaculture wetland in metropolitan areas, China: Characterization, bioavailability and probabilistic ecological risk. *Environ. Pollut.* **2023**, *324*, 121370. [[CrossRef](#)]
20. Chahouri, A.; Lamine, I.; Ouchene, H.; Yacoubi, B.; Moukrim, A.; Banaoui, A. Assessment of heavy metal contamination and ecological risk in Morocco's marine and estuarine ecosystems through a combined analysis of surface sediment and bioindicator species: *Donax trunculus* and *Scrobicularia plana*. *Mar. Pollut. Bull.* **2023**, *192*, 115076. [[CrossRef](#)]
21. Wang, Q.; Huang, X.; Zhang, Y. Heavy Metals and Their Ecological Risk Assessment in Surface Sediments of the Changjiang River Estuary and Contiguous East China Sea. *Sustainability* **2023**, *15*, 4323. [[CrossRef](#)]
22. Babasaheb, R.; Thorat, P.; Prasad, A.R. Heavy metal accumulation in a moderately polluted Ulhas estuary, Western India. *Reg. Stud. Mar. Sci.* **2023**, *60*, 102818. [[CrossRef](#)]
23. Fan, J.; Fan, D.; Wu, Y. Spatiotemporal variations of heavy metal historical accumulation records and their influencing mechanisms in the Yangtze River Estuary. *Sci. Total Environ.* **2023**, *854*, 158733. [[CrossRef](#)] [[PubMed](#)]
24. Filippi, G.; Dassenakis, M.; Paraskevopoulou, V.; Lazogiannis, K. Sediment quality assessment in an industrialized Greek coastal marine area (western Saronikos Gulf). *Biosciences* **2023**, *20*, 163–189. [[CrossRef](#)]
25. Ubonyaem, T.; Bureekul, S.; Charoenpong, C.; Luadnakrob, P.; Sompongchaiyakul, P. Preindustrial levels and temporal enrichment trends of mercury in sediment cores from the Gulf of Thailand. *Environ. Geochem. Health* **2023**, *45*, 4243–4256. [[CrossRef](#)] [[PubMed](#)]
26. Nishitha, D.; Amrith, V.N.; Arun, K.; Warriar, A.K.; Udayashankar, H.N.; Balakrishn, K. Study of trace metal contamination and ecological risk assessment in the sediments of a tropical river estuary, Southwestern India. *Environ. Monit. Assess.* **2022**, *194*, 94. [[CrossRef](#)] [[PubMed](#)]
27. Davis, R., Jr.; Welty, A.; Borrego, J.; Morales, J.A.; Pendon, J.G.; Ryan, J.G. Rio Tinto estuary (Spain): 5000 years of pollution. *Environ. Geol.* **2000**, *39*, 1107–1116. [[CrossRef](#)]
28. Borrego, J.; Morales, J.A.; Pendón, J.G. Holocene filling of an estuarine lagoon along the mesotidal coast of Huelva: The Piedras River mouth, southwestern Spain. *J. Coast. Res.* **1993**, *9*, 242–254.
29. Borrego, J. Sedimentología del estuario del río Odiel (Huelva, S.O. España). Ph.D. Thesis, Universidad de Huelva, Huelva, Spain, 1992.
30. CEDEX (Centro de estudios y experimentación de Obras Públicas). *Dinámica litoral de la flecha de El Rompido (Huelva)*; Ministerio de Obras Públicas: Madrid, Spain, 1991; p. 100.
31. CEEPYC (Centro de Estudios y Experimentación de Puertos y Costas 'Ramon Iribarren'). *Plan de Estudio de la Dinámica Litoral de la Provincia de Huelva*; Informe Dirección General de Puertos y Costas: Madrid, Spain, 1979; p. 37.
32. Cuenca, G.J. *Proyecto de Regeneración de Las Playas de Isla Cristina. Informe del Servicio de Costas*; Ministerio de Obras Públicas y Turismo: Madrid, Spain, 1991; p. 100.
33. Olías, M.; Cánovas, C.R.; Macías, F.; Basallote, M.D.; Nieto, J.M. The evolution of pollutant concentrations in a river severely affected by acid mine drainage: Río Tinto (SW Spain). *Minerals* **2020**, *10*, 598. [[CrossRef](#)]
34. Nelson, C.H.; Lamothe, P.J. Heavy metal anomalies in the Tinto and Odiel River and estuary system, Spain. *Estuaries* **1993**, *16*, 496–511. [[CrossRef](#)]
35. Arroyo, M.; Ruiz, F.; González-Regalado, M.L.; Rodríguez Vidal, J.; Cáceres, L.M.; Olías, M.; Campos, J.M.; Fernández, L.; Abad, M.; Izquierdo, T.; et al. Natural and anthropic pollution episodes during the Late Holocene evolution of the Tinto River estuary (SW Spain). *Sci. Mar.* **2021**, *85*, 113–123. [[CrossRef](#)]
36. Ruiz, F.; González-Regalado, M.; Borrego, J.; Morales, J.A.; Pendón, J.G.; Muñoz, J.M. Stratigraphic sequence, elemental concentrations and heavy metal pollution in Holocene sediments from the Tinto-Odiel Estuary, southwestern Spain. *Environ. Geol.* **1998**, *34*, 270–278. [[CrossRef](#)]
37. Muller, G. Index of Geoaccumulation in Sediments of the Rhine River. *J. Geol.* **1979**, *2*, 108–118.
38. Nocete, F. The first specialised copper industry in the Iberian peninsula: Cabezo Juré (2900–2200 BC). *Antiquity* **2006**, *80*, 646–657. [[CrossRef](#)]
39. Essalhi, M.; Sizaret, S.; Barbanson, L.; Chen, Y.; Lagroix, F.; Demory, F.; Nieto, J.M.; Sáez, R.; Capitán, M.A. A case study of the internal structures of gossans and weathering processes in the Iberian Pyrite Belt using magnetic fabrics and paleomagnetic dating. *Miner. Depos.* **2011**, *46*, 981–999. [[CrossRef](#)]
40. Arroyo, M.; Ruiz, F.; Campos, J.M.; Bermejo, J.; González-Regalado, M.L.; Rodríguez Vidal, J.; Cáceres, L.M.; Olías, M.; Abad, M.; Izquierdo, T.; et al. Where did Christopher Columbus start?: The estuarine scenario of a historical date. *Estuar. Coast. Shelf Sci.* **2021**, *250*, 107162. [[CrossRef](#)]
41. Lario, J.; Zazo, C.; Goy, J.L.; Dabrio, C.J.; Borja, F.; Silva, P.G.; Sierro, F.; González, A.; Soler, V.; Yll, E. Changes in sedimentation trends in SW Iberia Holocene estuaries (Spain). *Quat. Int.* **2002**, *93–94*, 171–176. [[CrossRef](#)]
42. Cabrera, F.; Conde, B.; Flores, V. Heavy metals in the surface sediments of the tidal river Tinto (SW Spain). *Fresen. Environ. Bull.* **1992**, *1*, 400–405. Available online: <https://hdl.handle.net/11441/134478> (accessed on 5 September 2023).
43. López-González, N.; Borrego, J.; Carro, B.; Soria-Lozano, O. Biodisponibilidad de Fe y metales pesados en los sedimentos de la ría de Huelva. *Geogaceta* **2005**, *37*, 219–222.

44. Ruiz, F.; Borrego, J.; González-Regalado, M.L.; López González, N.; Carro, B.; Abad, M. Impact of millennial mining activities on sediments and microfauna of the Tinto River estuary (SW Spain). *Mar. Pollut. Bull.* **2008**, *56*, 1258–1264. [[CrossRef](#)]
45. Abad, M.; Arroyo, M.; Ruiz, F.; González-Regalado, M.L.; Rodríguez Vidal, J.; Cáceres, L.M.; Toscano, A.; Gómez, P.; Gomez, G.; Romero, V. Miocene-Holocene paleoenvironmental changes in the Tinto River estuary (SW Spain) evidenced by sedimentology, geochemistry and fauna. *Carnets Geol.* **2022**, *22*, 825–845. Available online: <https://hdl.handle.net/10.2110/carnets.2022.2219> (accessed on 5 September 2023). [[CrossRef](#)]

Disclaimer/Publisher’s Note: The statements, opinions and data contained in all publications are solely those of the individual author(s) and contributor(s) and not of MDPI and/or the editor(s). MDPI and/or the editor(s) disclaim responsibility for any injury to people or property resulting from any ideas, methods, instructions or products referred to in the content.